The Plant Cell, Vol. 21: 3105–3118, October 2009, www.plantcell.org © 2009 American Society of Plant Biologists

YABBYs and the Transcriptional Corepressors LEUNIG and LEUNIG_HOMOLOG Maintain Leaf Polarity and Meristem Activity in *Arabidopsis* [W]

Melissa I. Stahle,[a,1] Janine Kuehlich,[a,2] Lindsay Staron,[b] Albrecht G. von Arnim,[b] and John F. Golz[a,c,3]

[a] Genetics Department, University of Melbourne, Parkville, VIC 3010, Australia
[b] Department of Biochemistry and Cellular and Molecular Biology, University of Tennessee, Knoxville, Tennessee 37996-0480
[c] Department of Biological Sciences, Monash University, Clayton, VIC 3800, Australia

In *Arabidopsis thaliana*, *FILAMENTOUS FLOWER* (*FIL*) and *YABBY3* (*YAB3*) encode YABBY domain proteins that regulate abaxial patterning, growth of lateral organs, and inflorescence phyllotaxy. In this study, we show that YABs physically interact with components of a transcriptional repressor complex that include LEUNIG (LUG), LEUNIG_HOMOLOG (LUH), the LUG-associated coregulator SEUSS, and related SEUSS-LIKE proteins. Consistent with the formation of a LUG-YAB complex, we find that *lug* mutants enhance the polarity and growth defects of *fil yab3* mutant leaves and that this enhancement is due to a loss of *LUG* activity from the abaxial domain. We performed a more extensive genetic analysis, which included the characterization of *yab* triple and quadruple mutants, *lug luh*/+ (heterozygous only for *luh*) mutants, and plants expressing artificial microRNAs targeting *LUG* or *LUH*. These analyses showed that the LUG-YAB complex also promotes adaxial cell identity in leaves as well as embryonic shoot apical meristem (SAM) initiation and postembryonic SAM maintenance. Based on the likely formation of the LUG-YAB complex in the abaxial domain of cotyledons and leaves, we propose that this complex has numerous non-cell-autonomous functions during plant development.

INTRODUCTION

Leaves of higher plants are typically polar structures with an asymmetric distribution of cell types along the proximodistal, lateral and adaxial (dorsal), and abaxial (ventral) axes. While adaxial and abaxial cells become morphologically distinct during later stages of leaf development, differences in the patterns of cell divisions and gene expression occur much earlier. This shows that organ polarity is established at, or just prior to, primordium emergence from the flanks of the shoot apical meristem (SAM).

In *Arabidopsis thaliana*, several families of transcription factors promote adaxial or abaxial cell identity in leaves and other lateral organs. The adaxial-promoting *PHABULOSA* (*PHB*), *PHAVOLUTA*, and *REVOLUTA* Class III homeodomain/leucine zipper transcription factors (*HD-ZIPIII*s) are expressed in the adaxial domain of lateral organs and the central region of the SAM. By contrast, members of the abaxial-promoting *KANADI* family (*KAN1-3*) are expressed in the abaxial domain of organs in a pattern that is complementary to the *HD-ZIPIII*s (Eshed et al., 2001; Kerstetter et al., 2001; McConnell et al., 2001; Otsuga et al., 2001; Emery et al., 2003). Based on the analysis of gain- and loss-of-function mutations in the *HD-ZIPIII*s and *KAN*s, it has been proposed that mutual antagonism between these classes of genes establishes organ polarity (McConnell and Barton, 1998; Eshed et al., 2001; McConnell et al., 2001; Emery et al., 2003).

In addition to the *KAN*s, several other factors promote abaxial cell identity. These include two members of the *AUXIN RESPONSE FACTOR* (*ARF*) family of transcription factors, *ETTIN* (*ETT*) and *ARF4* (Pekker et al., 2005) and the plant-specific *YABBY* (*YAB*) transcription factors (Sawa et al., 1999; Siegfried et al., 1999). Of the six members of YAB family in *Arabidopsis*, three (*FILAMENTOUS FLOWER* [*FIL*], also called *YAB1*, *YAB2*, and *YAB3*) are expressed in the abaxial domain of all lateral organs, whereas the other two (*CRABS CLAW* [*CRC*] and *INNER NO OUTER*) are restricted to the abaxial domains of carpels and the outer integument of ovules, respectively (Bowman and Smyth, 1999; Sawa et al., 1999; Siegfried et al., 1999; Villanueva et al., 1999). Due to the low levels of *YAB5* expression, transcript distribution has not been analyzed in detail. Loss of both *FIL* and *YAB3* results in narrow leaves and a partial loss of abaxial cell identity, whereas ectopic expression of *FIL*, *YAB3*, or *CRC* in leaves and petals causes partial abaxialization (Sawa et al., 1999; Siegfried et al., 1999; Eshed et al., 2001). *YAB*s also promote abaxial cell identity in other eudicot species, as mutations in *GRAMINIFOLIA*, the *Antirrhinum majus* ortholog of *Arabidopsis FIL*, result in pronounced adaxialization along the abaxial margin of leaves (Golz et al., 2004). In addition to a role in organ polarity, *YAB*s are also thought to promote lamina growth, perhaps by

[1] Current address: School of Molecular and Microbial Bioscience, University of Sydney, NSW 2006, Australia.
[2] Current address: Department of Biochemistry and Molecular Biology, University of Melbourne, Parkville, VIC 3010, Australia.
[3] Address correspondence to jgolz@unimelb.edu.au.
The author responsible for distribution of materials integral to the findings presented in this article in accordance with the policy described in the Instructions for Authors (www.plantcell.org) is: John F. Golz (jgolz@unimelb.edu.au).
[W] Online version contains Web-only data.
www.plantcell.org/cgi/doi/10.1105/tpc.109.070458

mediating communication between the adaxial and abaxial domains of the leaf (Eshed et al., 2004; Golz et al., 2004).

Although the precise regulatory relationship between the *YAB*s and the other gene families involved in polarity determination is poorly understood, it is likely that the YABs function as repressors based on their physical and genetic interactions with the *Antirrhinum* transcriptional corepressor STYLOSA (STY) (Navarro et al., 2004). While the STY ortholog in *Arabidopsis*, LEUNIG (LUG), is best known for its role in suppressing *AGAMOUS* expression during flower development (Liu and Meyerowitz, 1995; Conner and Liu, 2000), a recent study found that LUG and its associated coregulator SEUSS (SEU) also promote adaxial-abaxial patterning and growth of petals (Franks et al., 2002, 2006). This raises the possibility that LUG and SEU have a more general role in lateral organ patterning, possibly through interactions with the YABs.

To address this possibility, we characterized both physical and genetic interactions between the vegetatively expressed YABs, LUG, LEUNIG_HOMOLOG (LUH), and SEU. Using bioluminescence resonance energy transfer (BRET) assays, we show that a LUG-YAB complex is formed in planta. Subsequent mutant analysis in conjunction with a microRNA (miRNA)-based approach to diminish *LUG* activity revealed that the LUG-YAB complex promotes both adaxial and abaxial cell identity during leaf development. Defects in SAM initiation and maintenance are also observed when the components of this complex are removed. Based on the likely formation of the LUG-YAB complex in the abaxial domain of developing cotyledons and leaves, we propose that this complex regulates multiple signaling pathways that promote both adaxial cell identity in leaves and SAM initiation and maintenance.

RESULTS

Interactions between YAB Proteins and Components of the LUG Complex

Using the yeast two-hybrid system and a plate-based measure of α-Gal activity, we observed significant interactions between LUG and three of the four vegetatively expressed YABs (FIL, YAB3, and YAB5) (Table 1). Similar interactions were also observed between these YABs and LUH, which is consistent with LUG and LUH having similar biochemical properties. Subsequent analysis of FIL truncations revealed that the first 109 residues of the protein are required for LUG/LUH interactions (see Supplemental Table 1 online).

Given the importance of the coregulator SEU for LUG function (Franks et al., 2002; Sridhar et al., 2004), we examined whether YABs also interact with SEU in yeast. While DB-FIL fusions could not be tested due to strong autoactivation, both DB-YAB3 and DB-YAB5 induced α-Gal expression when coexpressed with AD-SEU. To extend this observation, we looked for interactions between the YABs and the three SEU-like proteins of *Arabidopsis* (SLK1-3; Franks et al., 2002), which also associate with LUG and LUH (see Supplemental Table 2 online). Consistent with biochemical redundancy among SEU and the SLKs, we find extensive interactions between all three SLKs and the YABs (Table 1), raising the possibility that SEU and SLKs are part of the LUG-YAB complex.

Table 1. Interactions between the YABs, Corepressors, and Associated Proteins in Yeast

	AD				
DB	Empty	FIL	YAB2	YAB3	YAB5
LUG	–[a]	+	–	++	++
LUH	–	++	–	+	++
	Empty	SEU	SLK1	SLK2	SLK3
YAB2	–	–	+	+	+
YAB3	–	++	+	++	++
YAB5	–	+	+	+	+
	Empty	FIL	YAB2	YAB3	YAB5
YAB2	–	–	+	–	+
YAB3	–	+	–	+	+
YAB5	–	+	+	+	+

[a]α-gal assay measuring activity of the LacZ reporter in three separate samples. Color change after 4 h (++), color change after 24 h (+), and no color change after 24 h (–).

Finally, we examined whether YABs form homodimers and YAB-YAB heterodimers in yeast as previous work has shown that FIL aggregates when expressed in vitro (Kanaya et al., 2002). In each self-self combination tested, a colormetric change was detected, indicating homodimerization. Similarly, heterodimerization was also observed, although only in some combinations (Table 1).

In Planta Detection of Protein–Protein Interactions

We next used the BRET assay to determine whether protein–protein interactions identified in yeast also occur in planta (Subramanian et al., 2004, 2006). BRET relies on the spectral shift from blue light emission to yellow light emission that occurs when the blue light–emitting *Renilla reniformis* luciferase (RLUC) is brought into close proximity to the yellow fluorescent protein (YFP). Coexpressing RLUC-LUG and either FIL-YFP or YFP-FIL in onion cells yielded an elevated yellow-to-blue (Y:B) ratio when compared with cells expressing RLUC-LUG and YFP alone, indicating interaction (Figure 1A). Finding that LUG is in close physical contact with FIL supports the hypothesis that LUG is in a complex with the YABs. An elevated Y:B ratio was also detected between RLUC-LUG and the YFP-SLK1 fusion protein, consistent with proposed biochemical redundancy between SEU and the SLKs (Figure 1B).

Interactions were also detected in cells coexpressing FIL-RLUC/YFP-FIL or YAB5-RLUC/YAB5-YFP, confirming that FIL and YAB5 form homodimers. Likewise, detection of interactions between YAB5-RLUC/FIL-YFP and YAB5-RLUC/YFP-FIL is consistent with heterodimerization (Figure 1C).

While elevated Y:B ratios were detected in some protein combinations, others such as those between YAB5 and either SLK1 or SLK2 did not generate elevated ratios (Figures 1A and 1B). While the BRET assay can be a robust technique for

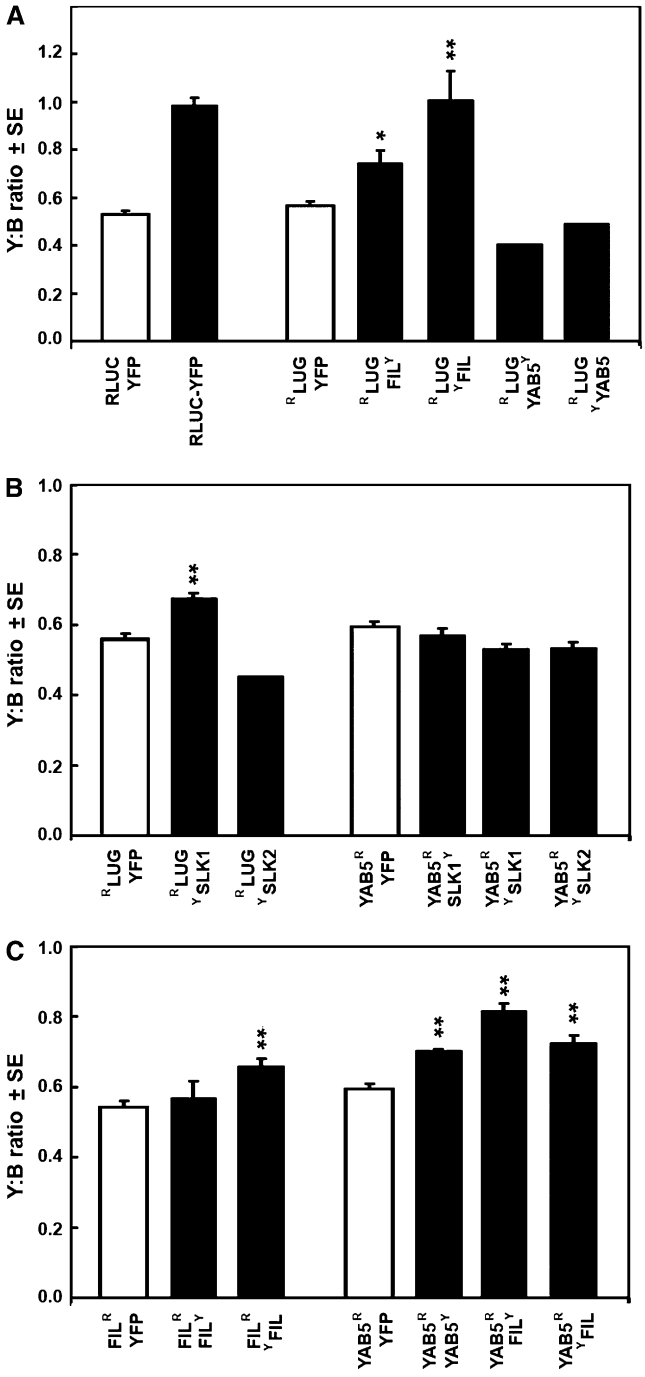

Figure 1. BRET Assays Detect Protein Interactions between LUG, YABs, and SLKs in Planta.

Y:B luminescence ratios from onion slices transiently coexpressing RLUC-LUG and the indicated YAB fusion protein **(A)**, RLUC-LUG or YAB5-RLUC, and the indicated SLK fusion protein **(B)** and FIL-RLUC or YAB5-RLUC, and the indicated YAB fusion protein **(C)**. The superscript letters R and Y indicate the positions of the RLUC and YFP tags, respectively. Results are means ± SE from at least three replicates, with the exception of LUG/YAB5 and LUG/SLK2 combinations, which were only repeated twice. Statistical difference from the RLUC-fusion/YFP control was calculated using a Student's *t* test, with $P < 0.01$ indicated by one asterisk and $P < 0.001$ indicated by two asterisks.

detecting protein–protein interactions in vivo, there are instances where BRET does not occur between interacting proteins (Subramanian et al., 2006), particularly if steric hindrance prevents the RLUC and YFP tags from coming within the critical distance of ~5 nm necessary for efficient energy transfer. Thus, negative BRET results do not rule out the possibility that these proteins interact. In summary, results from BRET assays largely support protein interactions detected in yeast.

lug Mutations Enhances the Vegetative Defects of *yab* Mutants

To determine the extent to which *YAB* function is dependent on LUG activity, we looked for synergistic interactions among *lug-1*, *seu-2*, and *fil-8 yab3-2* mutants. We found that the size of mature *fil yab3 lug* and *fil yab3 seu* rosette leaves was noticeably reduced when compared with *fil yab3* (Figures 2A to 2D; see Supplemental Table 3 online). As reduced growth was detected soon after leaf emergence (Figures 2E and 2F) and correlated with reduced activity of the cell cycle reporter $CYCB_{pro}$:*CYCB-β-GLUCURONIDASE* (*GUS*) (Figures 2G and 2H), we inferred that *lug* enhances the loss of cell proliferation in *fil yab3* plants.

In addition to reduced growth, *fil yab3 lug* also showed enhanced organ polarity defects. Examining the abaxial surface of *fil yab3 lug* mutants by scanning electron microscopy revealed larger and less irregular epidermal pavement cells than those of wild-type or *fil yab3* leaves (Figures 2I to 2K). Internally, the mesophyll tissue of *fil yab3 lug* leaves also appeared adaxialized in comparison to wild-type and *fil yab3* tissue, as abaxial cells were similar in shape to adaxial cells (Figures 2L to 2N).

Taking advantage of the *yab3-2* enhancer trap allele, which has a *GUS* reporter gene under the control of the *YAB3* promoter (Kumaran et al., 2002), we found that *YAB3* expression was slightly reduced in *fil yab3* leaves compared with morphologically wild-type *yab3* leaves, but greatly reduced and abaxially restricted in *fil yab3 lug* leaves (Figures 2O to 2Q). RNA in situ hybridization also detected an enlarged *PHB* expression domain in *fil yab3 lug* leaves relative to the wild type, consistent with adaxialization (Figures 2R and 2S).

Given that *LUG* is expressed broadly during plant development (Figures 3A and 3C; Conner and Liu, 2000), we next tested whether the observed synergism between *fil yab3* and *lug* mutations is due to a loss of the LUG-YAB complex from the abaxial side of the developing leaf. Using a *LUG*-targeting artificial miRNA (*amiR-LUG*; Figures 2T to 2V), we found that either constitutive or abaxial expression of the *amiR-LUG* in a *fil yab3* background produced a *fil yab3 lug* phenotype (Figures 2W and 2X), indicating that LUG activity in the abaxial domain of developing leaves is important for YAB function.

In addition to these observations, genetic interactions were also observed between *lug*, *fil*, and *yab3* mutations during flower development, suggesting that the function of the LUG-YAB complex is not restricted to the vegetative organs (see Supplemental Figure 1 online).

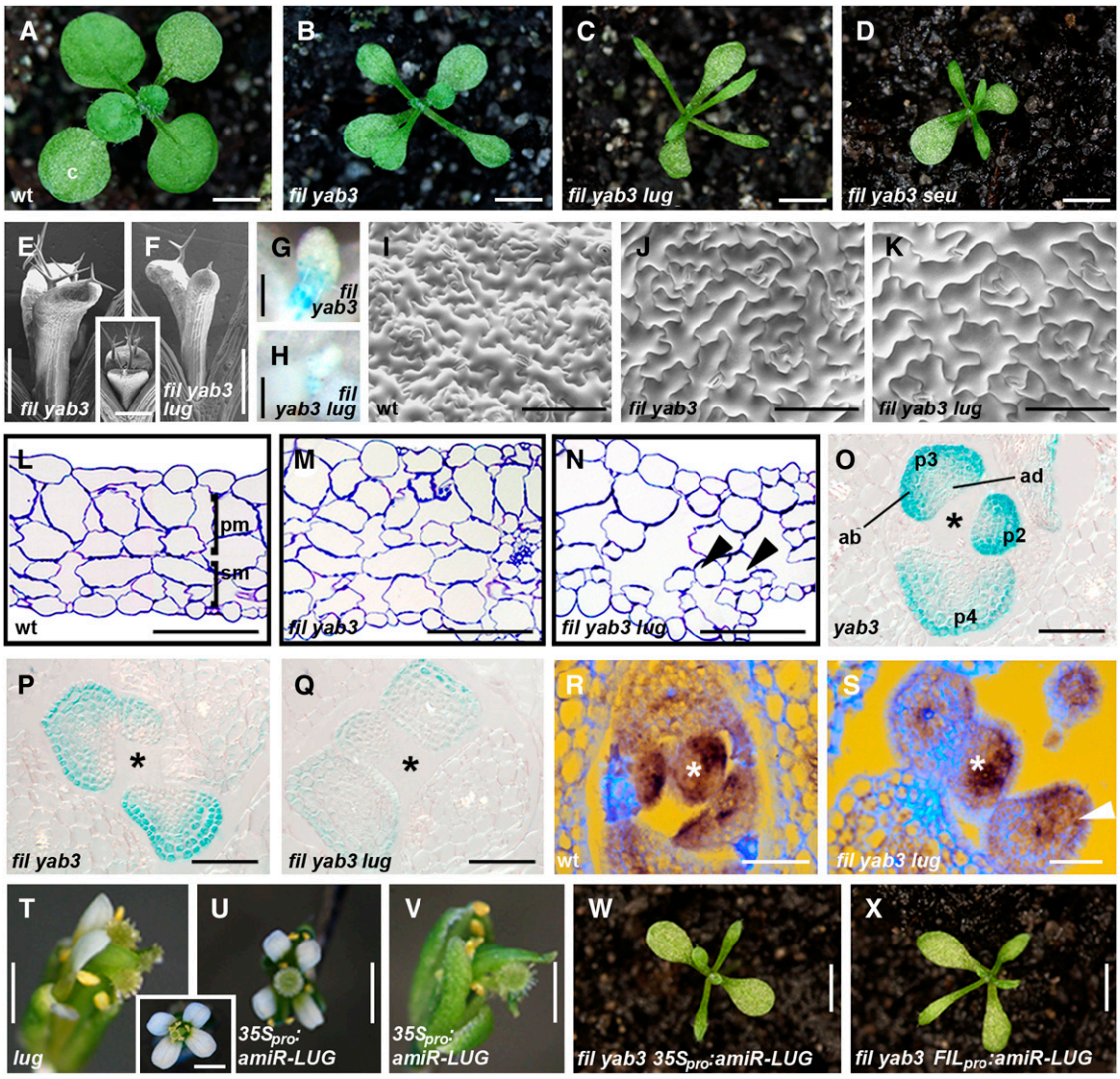

Figure 2. Enhancement of *fil yab3* Polarity Defects in *lug* and *seu* Mutant Backgrounds.

(A) to **(D)** Sixteen-day-old wild-type **(A)**, *fil-8 yab3-2* **(B)**, *fil-8 yab3-2 lug-1* **(C)**, and *fil-8 yab3-2 seu-2* **(D)** plants.
(E) and **(F)** Scanning electron micrographs of *fil-8 yab3-2* **(E)**, *fil-8 yab3-2 lug-1* **(F)**, and wild-type seedlings showing the first two leaves at an early stage of development.
(G) and **(H)** Expression of $CYCB1_{pro}$*:GUS* reporter in emerging leaves of *fil-5 yab3-1* **(G)** and *fil-5 yab3-1 lug-1* **(H)** mutants.
(I) to **(K)** Scanning electron micrographs showing the abaxial epidermis of fully expanded wild-type **(I)**, *fil-8 yab3-2* **(J)**, and *fil-8 yab3-2 lug-1* **(K)** leaves.
(L) to **(N)** Transverse sections through fully expanded wild-type **(L)**, *fil-8 yab3-2* **(M)**, and *fil-8 yab3-2 lug-1* **(N)** leaves. Arrowheads mark adaxialized spongy mesophyll cells.
(O) to **(S)** Distribution of *YAB3:GUS* (**[O]** to **[Q]**) and *PHB* RNA (**[R]** and **[S]**) in transverse sections of *yab3-2* **(O)**, *fil-8 yab3-2* **(P)**, *fil-8 yab3-2 lug-1* (**[Q]** and **[S]**), and wild-type **(R)** apices. Asterisks mark the position of the meristem, and arrowhead indicates expanded domain of *PHB* expression.
(T) *lug-444* and wild-type (inset) flowers.
(U) and **(V)** Representative flowers from $35S_{pro}$*:amiR-LUG* plants displaying an intermediate **(U)** and strong **(V)** *lug* mutant phenotype.
(W) and **(X)** Representative 16-d-old *fil-8 yab3-2* $35S_{pro}$*:amiR-LUG* **(W)** and *fil-8 yab3-2* FIL_{pro}*:amiR-LUG* **(X)** lines.
c, cotyledons; pm, adaxial palisade mesophyll cells; sm, abaxial spongy mesophyll cells; ad, adaxial side of primordia; ab, abaxial side of the primordia. Bars = 2 mm in **(A)** to **(D)**, **(W)**, and **(X)**, 1 mm in **(E)**, **(F)**, and **(T)** to **(V)**, and the inset in **(T)**, 200 μm in **(O)** to **(S)**, and 100 μm in **(G)** to **(N)**.

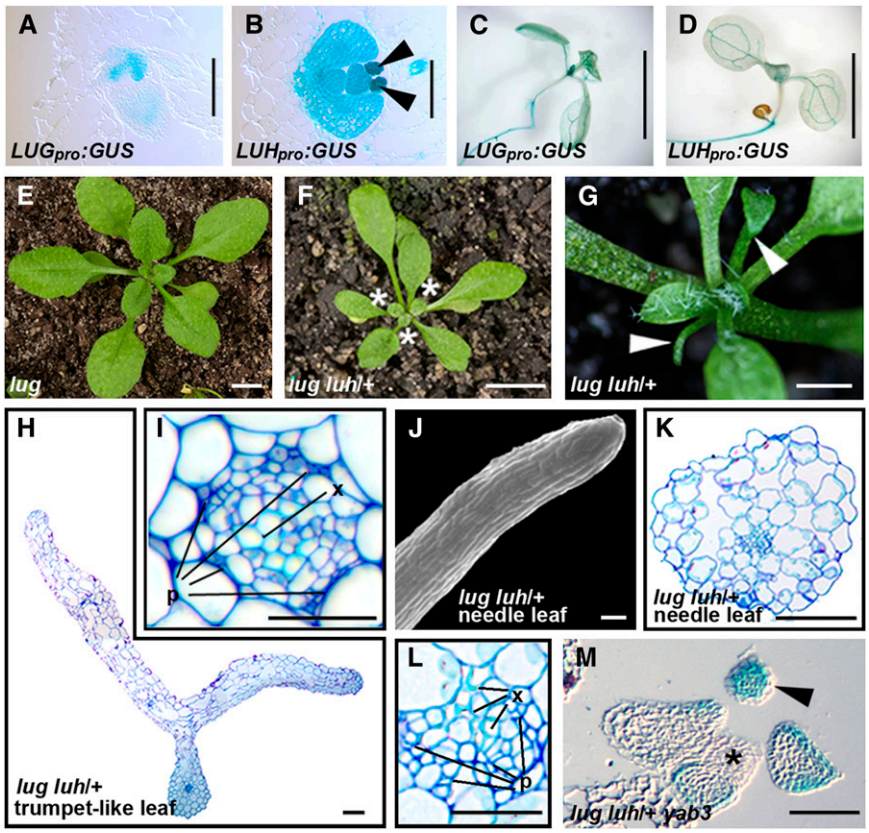

Figure 3. Leaf Polarity and Meristem Defects of *lug luh*/+ Plants.

(A) to **(D)** Histochemical localization *LUG$_{pro}$:GUS* (**[A]** and **[C]**) and *LUH $_{pro}$:GUS* (**[B]** and **[D]**) in 8-d-old plants viewed in transverse sections through the apex (**[A]** and **[B]**) or as whole mounts (**[C]** and **[D]**). Arrowheads indicate stipules.
(E) and **(F)** Twenty-eight-day-old *lug-444* **(E)** and *lug-444 luh-4*/+ **(F)** plants. *lug luh*/+ leaves are narrow and aberrant phyllotaxy is often observed (asterisks).
(G) *lug-444 luh-4*/+ plants with small needle-like and trumpet-shaped leaves (arrowheads).
(H) Transverse section through a mature *lug-444 luh-4*/+ trumpet-like leaf.
(I) Midrib vasculature of leaf shown in **(H)**. Position of phloem and xylem are indicated.
(J) Scanning electron micrograph of the epidermis of a *lug-444 luh-4*/+ needle-like leaf.
(K) and **(L)** Transverse section through a *lug-444 luh-4*/+ needle **(K)** and vasculature showing laterally displaced phloem **(L)**.
(M) Histochemical localization of *YAB3:GUS* in *yab3-2 lug-1 luh-4*/+ plant revealing ectopic *YAB3* expression in the adaxial domain of a needle-like leaf.
p, phloem; x, xylem. Bars = 5 mm in **(A)** and **(B)**, 2 mm in **(C)**, 200 μm in **(F)**, 100 μm in **(D)**, **(F)**, and **(G)**, and 20 μm in **(E)** and **(H)**.

Defects in Leaf Growth and Polarity Are Associated with *lug luh*/+ Mutants

Although LUG physically and genetically interacts with the YABs, there are no obvious leaf polarity defects associated with *lug* mutants. This may reflect redundancy between *LUG* and *LUH*, as promoters of both genes exhibited overlapping expression patterns when fused to the reporter GUS (Figures 3A to 3D). For instance, both *LUG* and *LUH* expression is detected throughout young developing leaves (Figures 3A and 3B), before being confined to the vasculature of older leaves (Figures 3C and 3D). As both *FIL* and *YAB3* are abaxially restricted, it is likely that the LUG-YAB complex forms in the abaxial domain of developing organs.

We next examined whether loss of both *LUG* and *LUH* activity results in leaf polarity defects as might be expected if these proteins regulate the YABs. Using likely null *lug* and *luh* mutant alleles (see Supplemental Table 4 and Supplemental Figure 2 online), we found that *lug luh* double mutants are embryonically lethal (data not shown; Sitaraman et al., 2008). However, leaf growth and patterning defects were apparent in plants homozygous for *lug* and heterozygous for *luh* (called *lug luh*/+) (cf. Figures 3E and 3F; see Supplemental Table 3 online; Sitaraman et al., 2008). These defects range from the petiole being displaced to the underside of the leaf to a complete loss of blade growth (Figure 3G, Table 2). Although variable in frequency, the polarity defects are nearly always confined to the first few leaves that arise following germination.

In trumpet-like leaves, disruptions to cell patterning were limited to the midrib, where the normal colateral vascular arrangement was replaced by phloem encircling xylem (Figures 3H and 3I). However, epidermal and mesophyll cell identity was

Table 2. Frequency of *lug luh*/+ Plants with Leaf Polarity Defects

Genotype[a]	Background	No. of Plants with: No Polarity Defects	Trumpet Leaves	Needle Leaves	Trumpet and Needle Leaves	Frequency of Polarity Defects
lug-012 luh-3/+	Col	18	5	2	3	35.7%
lug-012 luh-4/+	Col	81	59	19	22	55.2%
lug-444 luh-3/+	Col	33	8	1	1	23.3%
lug-444 luh-4/+	Col	27	6	2	0	22.9%

Col, Columbia.

[a]Twenty-day-old *lug luh*/+ plants identified in populations segregating for both *lug* and *luh* mutations were scored for polarity defects.

more severely affected in needle-like leaves (Figures 3J and 3K), although defects in vascular patterning were more variable (Figure 3L). These observations suggest that *lug luh*/+ leaves are partially abaxialized, an interpretation that is supported by the observed ectopic expression of *YAB3:GUS* in the adaxial domain of *lug luh*/+ *yab3-2* needle-like leaves (Figure 3M).

*YAB*s Act Redundantly in Promoting Adaxial Cell Identity

While the *lug luh*/+ leaves are partially abaxalized, it is not clear that these defects arise from altered YAB activity. We therefore investigated whether *YAB*s have a broader role in leaf patterning by examining the phenotypes of plants lacking not only *FIL* and *YAB3* activity, but also *YAB2* and *YAB5*. *yab2* and *yab5* mutants were obtained from the *Arabidopsis* stock center and their characterization showed that the both mutant alleles encode likely nonfunctional proteins (Figure 4A; see Methods). While neither single mutant has noticeable organ polarity defects, *yab5* mutants have considerably smaller leaves than the wild type (see Supplemental Table 3 online).

Of the mutant combinations examined, only *fil yab3 yab5* triple mutants and *fil yab2 yab3 yab5* quadruple mutants displayed significant differences from *fil yab3* (see Supplemental Figure 3 online for *fil yab2 yab3* mutants; note that when the triple and quadruple mutants showed identical phenotypes, only one of them is shown). For instance, 12% (n = 99) of *yab* triple mutants and 46% (n = 192) of *yab* quadruple mutants had three cotyledons (Figure 4B), whereas 9% (n = 192) of quadruple mutants had four cotyledons (Figure 4C). As the vasculature of each cotyledon joins the central vasculature of the hypocotyl, it is likely that the cotyledons have arisen separately during embryogenesis.

Triple and quadruple mutants also had short leaves that are either narrow or completely radialized (Figures 4D and 5E). Internally, spongy mesophyll tissue of narrow leaves extends around the leaf margin into the adaxial domain, and the adaxial palisade mesophyll tissue is centrally confined (Figure 4E). Consistent with abaxialization, phloem is adaxially displaced in some veins (Figure 4F). Surprisingly, vascular patterning is not severely affected in needle leaves, even though these organs lack adaxial/abaxial distinctions in the mesophyll (Figure 4G). Presence of *YAB3:GUS* staining throughout young needle-like leaves and restriction of *PHB* expression to the leaf vasculature (Figures 4H and 4I) are also consistent with abaxialization of triple mutant leaves. Similar defects are observed in *yab* quadruple mutants and thus are not shown. Given these similarities, it is likely that the polarity defects observed in *lug luh*/+ mutants reflect disruptions in the *YAB* pathway.

SAM Defects in Mutant Lines

yab mutants also display a range of meristem defects, with 10-d-old *fil yab3* meristems appearing flatter than wild-type meristems (Figures 5A and 5B). By contrast, SAMs of triple and quadruple *yab* mutants at a similar age lacked the distinctive anticlinal L2 cell layer that is normally seen in wild-type and *fil yab3* apices (Figure 5C shows the quadruple mutant; the triple mutant is identical). Unlike wild-type plants, both triple and quadruple *yab* mutants form ectopic axillary meristems in the axils of cotyledons (Figure 5D, arrow), which then go on to initiate secondary shoots as the plant matures (observed in 88% of *yab* quadruple mutants, n = 48; Figure 5E). Consistent with meristem dysfunction, approximately one-third of the primary and secondary shoots become noticeably fasciated (Figure 5E, arrowhead). As well as secondary shoots, additional shoots also arise from the adaxial surface of triple and quadruple *yab* mutant leaves (Figure 5F, asterisks), a phenomenon observed at low frequency in *fil yab3* mutants (Kumaran et al., 2002).

While presence of secondary shoots from cotyledon axils was not a feature of *lug luh*/+ mutants, SAM defects were also apparent in this line. In comparison to *lug* mutant apices, which are similar to the wild type, 14-d-old *lug luh*/+ SAMs were broader and lacked strict anticlinal cell divisions in the L2 layer (Figures 5G and 5H). Consistent with an increased size of *lug luh*/+ apices, *STM* expression was expanded when compared with wild-type apices (Figures 5I and 5J) and fasciation often occurred following the transition to flowering (Figures 5K and 5L; *lug-444 luh-3*/+ 61%, n = 61; *lug-444 luh-4*/+: 45%, n = 51). Internally, fasciated inflorescences were significantly broader and flatter than *lug* apices (Figures 5M and 5N).

Role of the YAB-LUG Pathway in Regulating Early SAM Development

We reasoned that more profound defects in SAM development were likely to arise if the activity of the LUG-YAB complex was severely compromised. To test this possibility, we generated *fil lug luh*/+ and *fil yab3 lug luh*/+ mutant combinations. Despite

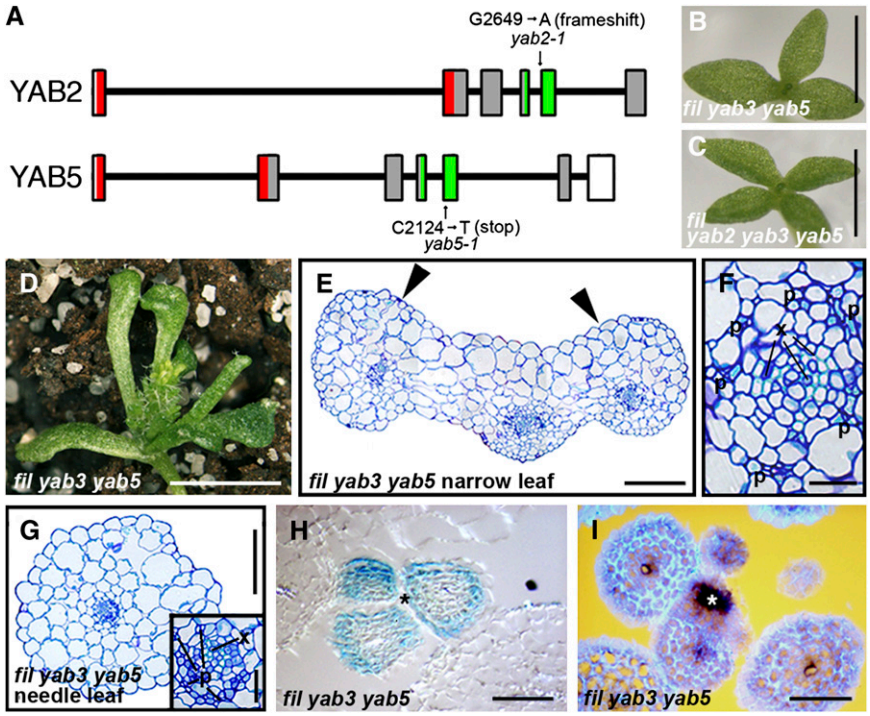

Figure 4. Vegetative Phenotypes of *yab* Triple and Quadruple Mutants.

(A) Structure of the *YAB2* and *YAB5* genes. Boxes depict the 5′ and 3′ untranslated regions (white), Zn-finger domain (red), and YABBY domain (green). The position of the point mutations (arrows) is measured from the start ATG of the genomic sequence.
(B) and **(C)** Polycotyledonous *fil-8 yab3-2 yab5-1* **(B)** and *fil-8 yab2-1 yab3-2 yab5-1* **(C)** seedlings.
(D) *fil-8 yab3-2 yab5-1* mutants with narrow or radial leaves.
(E) Transverse section through a narrow *fil-8 yab3-2 yab5-1* leaf. Normal palisade and spongy mesophyll tissue is present between arrowheads.
(F) Vasculature of leaf shown in **(E)** showing phloem surrounding central xylem tissue.
(G) Transverse section through a radial *fil-8 yab3-2 yab5-1* leaf and associated vasculature (inset).
(H) and **(I)** Distribution of GUS activity (from *YAB3:GUS*) **(H)** and *PHB* RNA **(I)** in transverse sections of *fil-8 yab3-2 yab5-1* apices. Asterisks mark the position of the meristem.
Bars = 2 mm in **(B)** to **(D)**, 100 μm in **(E)** and **(G)**, 50 μm in **(H)** and **(I)**, and 20 μm in **(F)** and the inset in **(G)**.

moderate linkage between *FIL* and *LUH*, both mutant classes were identified at low frequency in segregating populations and, consistent with a greater affect on SAM development, had extremely narrow cotyledons and inactive SAMs (Figure 6A shows the triple mutant). Unlike *lug luh*/+ apices, which only have defective cell division in the L2 layer of the SAM, divisions in both L1 and L2 cell layers of *fil lug luh*/+ and *fil yab3 lug luh*/+ apices were disrupted, resulting in a loss of SAM organization (Figures 6B to 6D). Some cytoplasmically dense cells were still present in these meristems, although they were arranged randomly within the central region of the apex (Figure 6D). As these defects were apparent in 4-d-old meristems, it is likely that they reflect alterations in embryonic SAM formation.

By ~10 d after germination, meristem activity was restored in all *fil lug luh*/+ and most *fil yab3 lug luh*/+ apices, and the structure of these reestablished SAMs was indistinguishable from that of *lug luh*/+ mutants (Figure 5H). Leaves arising from these meristems had more severe growth and polarity defects relative to *fil yab3* and *lug luh*/+ mutants, with many *fil yab3 lug luh*/+ leaves being radial (Figure 6E). Analysis of the polarity defects in these leaves suggested disruptions to both adaxial and abaxial cell identities (see Supplemental Figure 4 online).

Given the obvious enhancement of SAM defects when mutations in *YAB*s and corepressors mutants are combined, we hypothesized that the LUG-YAB complex regulates SAM development via a signaling pathway active in developing cotyledons and leaves. Consistent with this model, we found coexpression of *LUG*, *LUH*, and *FIL* in developing cotyledons as well as leaves (see Supplemental Figure 5 online). To test this model directly, we examined the effect on SAM development when the activity of both *LUG* and *LUH* is removed from developing leaves. Transgenic plants expressing *amiR-LUG* under the control of the organ-specific *AS1* promoter were crossed to *luh* mutants and their progeny examined for SAM defects. *luh AS1*$_{pro}$*>>amiR-LUG* (see Methods for description) seedlings identified in segregating populations had broad SAMs that produced one or two leaf primordia before becoming inactive (Figure 6F). Internally, the structure of these SAMs was similar to the wild type, although cells lacked the dense cytoplasm that is characteristic feature of actively dividing cells of wild-type meristems (Figure 6G). This

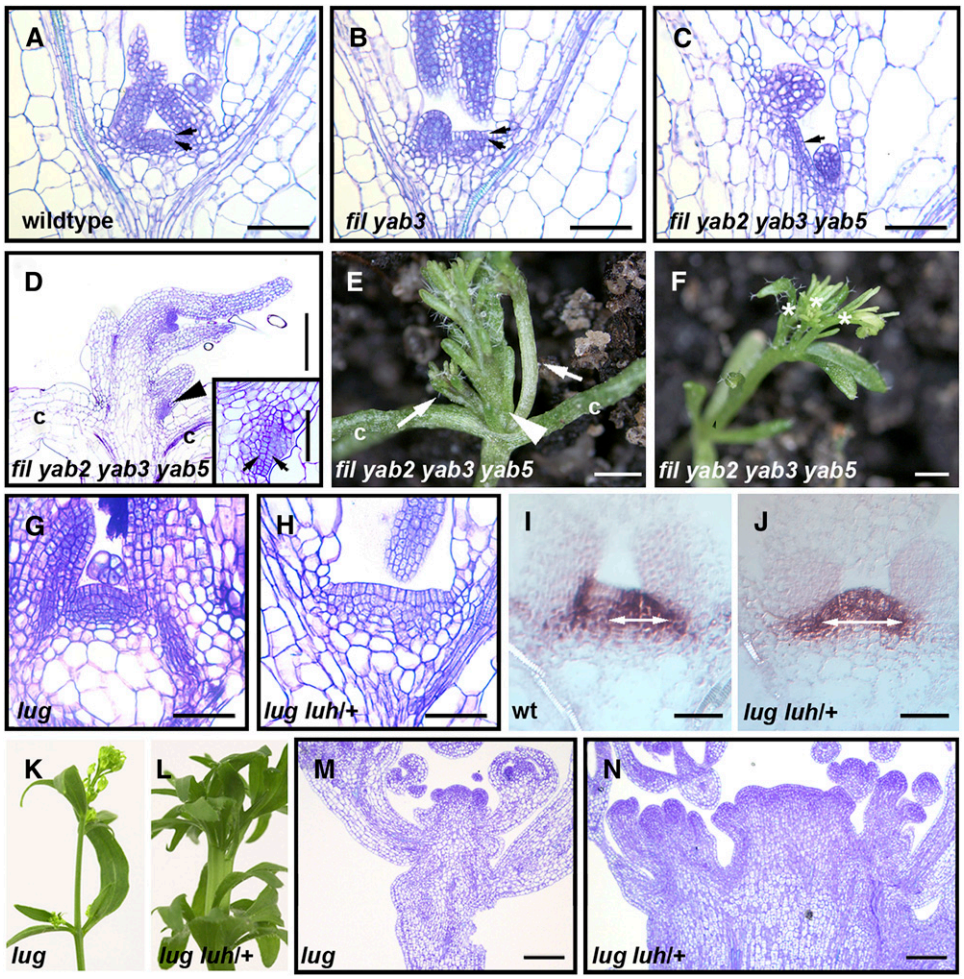

Figure 5. SAM Defects of *yab* and *lug luh*/+ Mutants.

(A) to **(C)** Longitudinal sections through apices of 10-d-old short-day-grown *yab2-1 yab3-2 yab5-1* **(A)**, *fil-8 yab3-2* **(B)**, and *fil-8 yab2-1 yab3-2 yab5-1* **(C)** mutant plants. Arrows indicate anticlinal L1 and L2 cell layers.

(D) Section through a quadruple *yab* mutant showing the establishment of a secondary shoot SAM (arrowhead) in the axil of a cotyledon (c). Inset: close-up of secondary shoot meristem with clear L1 and L2 anticlinal cell layers (arrows).

(E) *fil-8 yab2-1 yab3-2 yab5-1* quadruple mutant showing a fasciated primary shoot (arrowhead) and two secondary shoots (arrows) arising from the axils of cotyledons (c).

(F) Formation of ectopic meristems from the adaxial surface of a *yab* quadruple mutant leaf (asterisks).

(G) and **(H)** Section through apices of 14-d-old short-day-grown *lug* **(G)** and *lug-444 luh-4*/+ **(H)** plants.

(I) and **(J)** RNA in situ hybridization using *STM* as a probe on wild-type **(I)** and *lug-444 luh-4*/+ **(J)** apical sections.

(K) and **(L)** Inflorescences of *lug-444* **(K)** and *lug-444 luh-4*/+ **(L)**.

(M) and **(N)** Sections through of *lug-444* **(M)** and *lug-444 luh-4*/+ **(N)** inflorescences.

Bars = 1 mm in **(E)** and **(F)**, 200 μm in **(D)**, 100 μm for **(M)** and **(N)**, and 50 μm in **(A)** to **(C)**, **(G)** to **(J)**, and the inset in **(D)**.

finding shows that *LUG* and *LUH* function non-cell-autonomously and is consistent with the LUG-YAB complex promoting SAM development via a leaf-based signaling pathway.

Embryonic Defects of *seu slk2* Mutants

Further characterization of the embryonic SAM defects of *fil lug luh*/+ and *fil yab3 lug luh*/+ mutants was not possible due to rarity of such seeds in siliques segregating for these mutations. To circumvent this problem, we examined whether mutations in other components of the LUG-YAB complex have embryonic SAM defects. We focused on *SEU* and the *SLK*s, as yeast two-hybrid assays and expression analyses suggest that these genes may function redundantly (see Supplemental Table 2 online; Figure 7A).

Given that protein alignments and phylogenetic analysis suggested that SLK2 is more closely related to SEU than either SLK1 or SLK3 (Figure 7B), we introgressed *slk2* T-DNA mutants

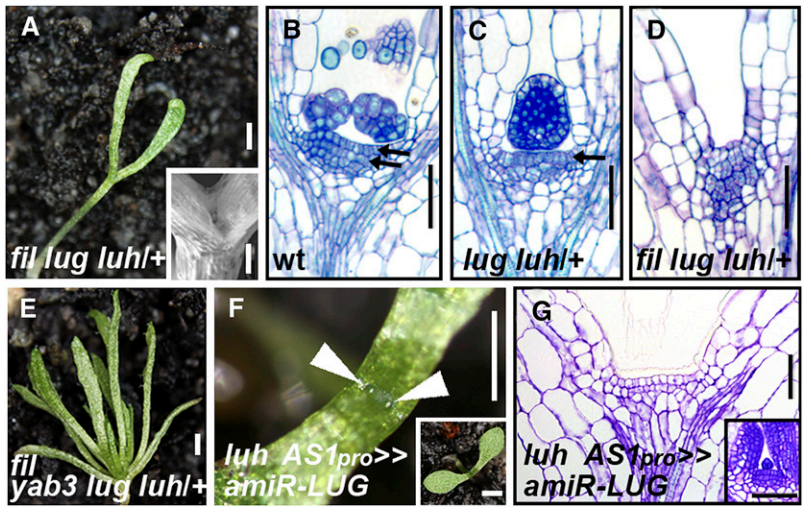

Figure 6. Genetic Interactions between Corepressor and *YAB* Mutants Reveal a Role in Embryonic SAM Development.

(A) Six-day-old *fil-8 lug-1 luh-3*/+ plants lack a SAM. Inset: scanning electron micrograph of shoot apex.
(B) to **(D)** Longitudinal sections through apices of 4-d-old wild-type **(B)**, *lug-1 luh-3*/+ **(C)**, and *fil-8 lug-1 luh-3*/+ **(D)** seedlings. Layers in which cells are dividing anticlinally are indicated with arrows. Note the absence of a layered SAM structure in *fil-8 lug-1 luh-3*/+ plants.
(E) A 30-d-old *fil-8 yab3-2 lug-1 luh-3*/+ plant with extremely narrow and needle-like leaves.
(F) SAM of a 16-d-old *luh-4 AS1*$_{pro}$*>>amiR-LUG* plant is inactive, but signs of organ formation are apparent (arrows). Inset: view of entire seedling.
(G) Section through a terminated *luh-4 AS1*$_{pro}$*>>amiR-LUG* apex revealing the absence of cytoplasmically dense cells. Inset: view of a wild-type apex with cytoplasmically dense cells.
Bars = 1 mm in **(A)** to **(E)** and the inset in **(F)**, 500 μm in **(F)**, and 50 μm in **(B)** to **(D)** and **(G)**.

into a *seu* background (see Methods; see Supplemental Figure 2 online). Consistent with functional redundancy, we found that *seu* mutants heterozygous for *slk2* (called *seu slk2*/+) had enhanced floral defects when compared with *seu* mutants. This included a reduction in floral organ number and size and the formation of prominent stigmatic horns, all characteristic features of *lug* mutant flowers (Figures 7C to 7E). This phenotypic enhancement shows that *SLK2* functions with *SEU* in *LUG*-regulated processes during flower development.

Genotyping showed that all *seu slk2* double mutants lacked a SAM and had cotyledons that were both reduced in size and frequently fused (Figure 7F). Internally, there was a complete absence of cytoplasmically dense cells and no evidence of SAM formation (Figure 7G). Using differential interference contrast (DIC) optics to follow embryo development in developing *seu*/+ *slk2* siliques, we found that ~25% of heart-staged embryos had reduced cotyledons and lacked the stereotypical pattern of cell divisions that occur in the apical regions of the phenotypically wild-type *slk2* mutant embryos (Figures 7H and 7I). Both the frequency of occurrence and the cotyledon defects suggested that these aberrant embryos are *seu slk2* mutants. We next examined expression of the meristem-specific gene *CLV3* in *seu slk2* embryos by introgressing a *CLV3*$_{pro}$*:YFP-ER* reporter into the *seu*/+ *slk2* mutant background. Consistent with a lack of SAM formation, we were unable to detect *CLV3* expression in heart-stage embryos with a *seu slk2* phenotype (Figures 7J and 7K).

Finally, we introduced a constitutively expressed amiRNA that targets *LUH* (*35S*$_{pro}$*:amiR-LUH*) into a *lug*/+ background and found meristemless progeny in population derived from six independent lines. Genotyping confirmed that these seedlings were *lug 35S*$_{pro}$*:amiR-LUH* (Figure 7L). Sections through the apex of these seedlings were similar to those of *seu slk2* (Figure 7M) in that there was a complete absence of cytoplasmically dense cells and no evidence of SAM formation, supporting the notion that the LUG-YAB pathway is required for the initiation of embryonic SAM development.

DISCUSSION

YABs Are Part of a Multicomponent Regulatory Complex

Based on studies in *A. majus*, it has been proposed that the transcriptional corepressor STY regulates YAB activity (Navarro et al., 2004). Using yeast and BRET assays, we show that these interactions are conserved in *Arabidopsis* and thus are likely to be important for *YAB* function in other eudicots. As well as interacting with the corepressor LUG and related LUH protein, we show that *Arabidopsis* YABs may also interact with the coregulator SEU and related SLKs proteins. Given that SEU is a known component of the LUG complex (Sridhar et al., 2004; Sitaraman et al., 2008) and that SLKs are likely to share this function (this study), we propose that YABs are part of a multicomponent complex that includes a corepressor (LUG or LUH) and a coregulator (SEU or a SLK protein) (Figure 8A). Furthermore, as YABs are also capable of forming homo- or heterodimers, it is probable that this complex includes more than one YAB protein.

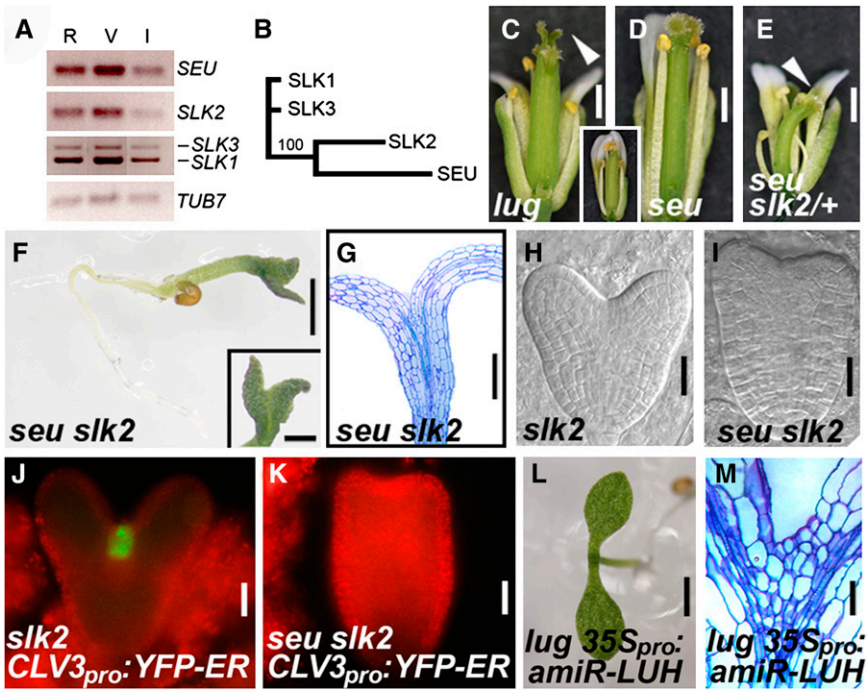

Figure 7. Phenotypes of *seu slk2*/+ and *seu slk2* Mutants.

(A) RT-PCR expression analysis of *SEU*, *SLK1-3*, and the tubulin gene *TUB7* in roots, vegetative shoot, and inflorescence tissue. *SLK1* cDNA is distinguished from *SLK3* cDNA following digestions with *Hpa*I (see Methods).
(B) Phylogeny of the *Arabidopsis* SEU/SLK family of coregulators. The tree was constructed by the neighbor-joining method and bootstrap values are indicated.
(C) to **(E)** Flowers of *lug-444* **(C)**, *seu-4* **(D)**, and *seu-4 slk2-1*/+ **(E)** mutants with several outer whorl organs removed to reveal the carpel. Inset is a wild-type flower. Arrowheads indicate stigmatic horns.
(F) Twenty-eight-day-old *seu-4 slk2-1* double mutants lack an active SAM. View of the shoot apex reveals fusion between cotyledons (inset).
(G) Longitudinal section through a 14-d-old *seu-4 slk2-1* shoot apex revealing a complete absence of cytologically dense cells typical of an active SAM.
(H) and **(I)** DIC microscopy of *slk2* **(H)** and *seu slk2* **(I)** embryos at the heart stage of development.
(J) and **(K)** $CLV3_{pro}$*:YFP-ER* marker expression in *slk2* **(J)** and *seu slk2* **(K)** embryos at the heart stage of development. Note the complete absence of YFP florescence in *seu slk2* double mutant embryos.
(L) *lug-444* $35S_{pro}$*:amiR-LUH* plants lack a SAM.
(M) Section of a *lug-444* $35S_{pro}$*:amiR-LUH* plants revealing the absence of cytoplasmically dense cells.
Bars = 1 mm in **(F)** and **(L)**, 0.5 mm in **(C)** to **(E)** and the inset in **(F)**, 200 μm in **(G)**, 50 μm in **(M)**, and 20 μm in **(H)** to **(K)**.

Genetic analysis provides support for the formation of a LUG-YAB regulatory complex. For instance, *lug luh*/+ mutants display polarity and meristem defects that can be explained, at least in part, by disruptions in the *YAB* pathway. In addition, *lug* and *seu* mutants enhance the growth and abaxial polarity defects of *fil yab3* leaves. This enhancement becomes more pronounced when *fil yab3* mutants are combined with *lug luh*/+, leading to disruptions in embryonic SAM formation. Finally, we show that reduced *LUG* activity in the abaxial domain of developing *fil yab3* leaves causes a *fil yab3 lug* leaf phenotype. In addition to regulating leaf polarity and meristem activity, our analysis indicates that *LUG* functions with the *YAB*s to prevent *KNOX* expression in leaves (see Supplemental Figure 6 online). Taken together, these data make a compelling case for the formation of a LUG-YAB complex in the abaxial domain of developing cotyledons and lateral organs. Based on the vegetative and SAM defects associated with mutations in LUG and LUH, this study has expanded the known functions of the corepressors and further underscored their importance as general regulators of plant development.

Function of YABs in the LUG Complex

Although FIL binds DNA in vitro, it displays no sequence specificity (Kanaya et al., 2002). If this observation applies equally to the other YABs, it is unlikely that YABs recruit LUG or LUH to specific sites within the genome. We therefore favor a model in which the LUG-YAB complex is recruited to promoter elements via interactions with transcription factors bound to SEU or SLKs (Figure 8A). What then is the function of YABs within the LUG complex? One possibility is that the YABs recruit factors involved in long-term transcriptional regulation, such as chromatin-modifying enzymes or, alternatively, the YABs might enhance the stability of the LUG-SEU transcription factor complex when

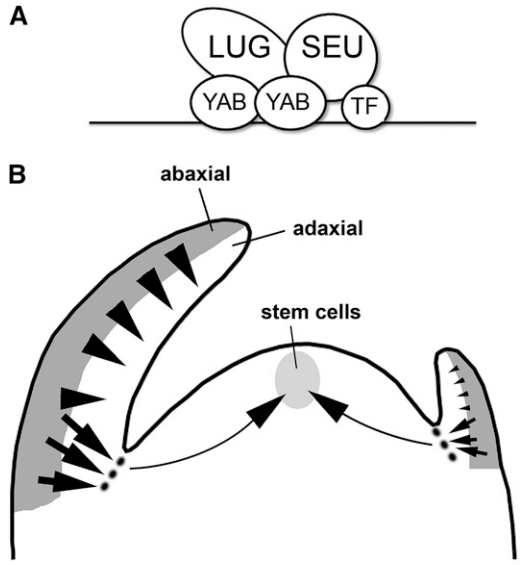

Figure 8. Proposed Composition of the LUG-YAB Complex and Its Role in Signaling during Vegetative Development.

(A) Based on protein–protein interactions in yeast and in planta, it is likely that the LUG-YAB complex includes two YAB proteins (forming either homodimers or heterodimers) in close association with LUG or LUH and SEU or one of the three SLKs. According to our model (see text for details), the LUG-YAB complex is recruited to specific *cis*-regulatory elements (black line) by SEU-interacting transcription factors (TF).

(B) Given the expression patterns of *LUG*, *LUH*, and *FIL*, it is likely that the LUG-YAB complex forms in the abaxial domain of developing cotyledons and leaves (shaded). Once formed, this complex activates two signaling pathways. The first promotes adaxial cell identity (arrowheads) and the other regulates SAM initiation and maintenance (arrows) possibly by promoting boundary formation (dotted line).

bound to DNA. Current work is aimed at distinguishing between these possibilities.

The *YAB* Pathway Promotes Adaxial Cell Identity

The absence of *PHB* expression in the mesophyll tissue of triple *yab* mutants leaves suggests that these organs have lost adaxial cell identity. This finding, together with previous work showing a minor loss of adaxial cell identity *kan1 kan2* mutants leaves (Ha et al., 2007), raises the intriguing possibility that establishment of adaxial cell identity is dependent on the correct specification of abaxial cell identity. Several lines of evidence argue against such a relationship. First, severe loss of abaxial cell identity in leaves of *kan* triple mutants is not associated with a loss of *PHB* expression (Eshed et al., 2004). Second, detecting *YAB3* expression in *yab* triple mutants leaves clearly shows that these organs retain abaxial cell identity. Given this, we propose that *YAB*s play a more direct role in promoting adaxial cell identity, although how this is achieved is currently not understood. As adaxial regulators, *YAB*s are unique in being expressed predominantly in the abaxial domain of lateral organs in divergent eudicots (Bowman and Smyth, 1999; Siegfried et al., 1999; Kim et al., 2003; Eshed et al., 2004; Golz et al., 2004). Furthermore, as YAB proteins accumulate abaxially (Navarro et al., 2004; Goldshmidt et al., 2008), we propose that the YABs promote adaxial cell identity non-cell-autonomously (Figure 8B). Such a function is not unprecedented, as previous studies have hinted at such functions during floral development (Alvarez and Smyth, 1999; Bowman and Smyth, 1999; Villanueva et al., 1999; Goldshmidt et al., 2008; Prunet et al., 2008).

Given the redundant role of *FIL* and *YAB3* in promoting abaxial cell identity, it is perhaps surprising that further loss of *YAB* activity (loss of *YAB2*, *YAB5*, or both) does not cause a more pronounced loss of abaxial cell identity. In fact, the only evidence that *YAB2* and *YAB5* promote abaxial cell identity comes from mild adaxialization observed in *fil*/+ *yab2 yab3 yab5* leaves (see Supplemental Figure 3 online). There are several possible explanations for this observation. First, it may simply be that *YAB2* and *YAB5* do not promote abaxial cell identity, perhaps due to a loss of this function over evolutionary time. Equally possible is that the abaxial-promoting activity of the YABs is an evolutionary-derived function that has been acquired by FIL/YAB3 but not YAB2 or YAB5. Consistent with *YAB*s originally being adaxial determinants, at least one *YAB* gene is expressed adaxially in the basal angiosperm *Amborella trichopoda* (Yamada et al., 2004).

Alternatively, the abaxial function may be masked by factors that act redundantly with the *YAB*s. Candidates include the *KAN*s, which are known to function with the *YAB*s in leaf development (Eshed et al., 2004), and the related *ARF*s, *ETT* and *ARF4*. One way to distinguish between these possibilities is to examine whether YAB2 and YAB5 share the same or different gene targets as those of FIL/YAB3. If the analysis of gene targets is extended to the KANs and ETT/ARF4, it will be possible to determine the extent of redundancy both within the *YAB* family and between *YAB*s and other polarity determinants.

The Importance of Boundaries for *YAB* Function

The involvement of the LUG-YAB complex in promoting embryonic SAM development and postembryonic maintenance reflects a further non-cell-autonomous function. This may be related to the recently identified role for short-range YAB signaling in regulating phyllotaxis, primordia growth, and SAM activity (Goldshmidt et al., 2008). Genetic analysis indicates that these functions are largely dependent on *LATERAL SUPPRESSOR* (*LAS*), a gene that is expressed at the boundary between lateral organs and the SAM (Greb et al., 2003). The precise relationship between the *YAB*s and the organ boundary is presently not clear, but an attractive scenario is that the YAB signal induces a signaling cascade or secondary messenger upon reaching the organ/SAM boundary (Goldshmidt et al., 2008). Alternatively, the primary function of the YABs may be to promote boundary formation and that the non-cell-autonomous functions ascribed to the YAB signal are in fact those of the boundary. Finding *LAS* expression is altered in *yab* mutants and in lines overexpressing *FIL* is consistent with *YAB*s regulating boundary specification (Goldshmidt et al., 2008). If YABs do indeed perform this function, it might be expected that further disruptions to the LUG-YAB complex might cause phenotypes associated with boundary disruption. The best-studied boundary genes are those belonging

to the *CUP-SHAPED COTYLEDON* (*CUC*) family of transcription factors; mutations in which cause a loss of embryonic SAM formation and cotyledon fusion (Aida et al., 1997; Takada et al., 2001; Vroemen et al., 2003). Although not a complete phenocopy of *cuc1 cuc2* mutants, presence of fused cotyledons in *seu slk2* mutants, together with the loss of the embryonic SAM, suggests that the LUG-YAB complex may regulate *CUC* activity. Given that *LAS* has been placed downstream of the *CUCs* in the genetic hierarchy regulating axillary meristem formation (Hibara et al., 2006), it is possible that YABs regulate *LAS* via the *CUC*s. Future work will therefore need to address the precise regulatory relationship between the LUG-YAB complex and genes involved in boundary formation.

METHODS

Plant Material and Genetics

Arabidopsis thaliana mutants used in this study and their backgrounds are listed (see Supplemental Table 4 online). Where genetic interactions involved a mixed Columbia/Landsberg *erecta* background, the mutant phenotypes of F2 or F3 plants were shown to be independent of the *erecta* mutation. Insertion sites for the *lug-444*, *lug-012*, *luh-4*, *slk2-1*, and *slk2-2* T-DNA insertion alleles were confirmed by PCR using oligonucleotides specific for each line and by sequencing across the insertion site. Genomic DNA spanning the *YAB2* and *YAB5* loci was sequenced to confirm the presence of the ethyl methanesulfonate–induced mutations in *yab2-1* and *yab5-1* plants. The *yab2-1* mutation abolishes the annotated splice acceptor site for the 4th intron, leading to a cryptic site just downstream of the mutation being used for splicing. Sequencing reveals an extra nucleotide the *yab2* mutant transcript, leading to the conserved YABBY DNA binding domain being replaced with 35 unrelated amino acids as a result of the frame shift. Similarly, *yab5-1* is predicted to encode a truncated protein lacking most of the YABBY domain. Double, triple, and higher-order *yab* mutant combinations were identified in segregating F2 or F3 families and genotyped to confirm identity. Primers and PCR conditions are available upon request. LUG_{pro}*:GUS* and LUH_{pro}*:GUS* reporter lines were generated by cloning the 3- and 2-kb intergenic region upstream of their respective annotated open reading frames into a GUS-containing pRITA vector (a gift from John Bowman, Monash University, Australia). The promoter:GUS cassette was subcloned into the binary vector pMLBART (Gleave, 1992) and introduced into *Agrobacterium tumefaciens* (GV3101) by electroporation. Transgenic *Arabidopsis* plants (Columbia background) were generated using an *Agrobacterium* floral dip procedure (Clough and Bent, 1998) and identified following treatment with BASTA. Plants were either grown on soil or on 0.5× Murashige and Skoog media in a growth room at 18°C or growth cabinet kept at 21°C under lights for 8 h (short days) or 16 h (long days).

Yeast Two-Hybrid Assays

LUG, *LUH*, *SEU*, *SLK1-3*, and *YAB* coding sequences were amplified from vegetative cDNA using a high-fidelity Taq polymerase and cloned into pGBK-T7 and pGAD-T7 (Clontech) vectors. The suffix DB and AD were give to fusions protein produced from pGBK-T7 and pGAD-T7, respectively. FIL truncations were generated by PCR using the *FIL* cDNA as a template and cloned into pGAD-T7. Constructs were transformed separately into yeast and then mated according to the manufacturer's instructions (Clontech). Interactions between fusion proteins were assessed by growth and an α-Gal plate-based colorimetric assay according to published protocols. Interactions were assessed after 4, 24, and 36 h.

BRET Analysis

Proteins used in the BRET assay were cloned downstream of the *35S* promoter and in frame with RLUC or YFP at the N or C terminus. Plasmid DNA containing these fusions constructs were then introduced into adaxial onion epidermal tissue using particle bombardment as described previously (Subramanian et al., 2004, 2006). Following incubation, onion tissue was submerged in 10 μM coelenterazine to excite RLUC and BRET measurements taken with a TD 20/20 luminometer fitted with a dual-color accessory (Turner Designs) using previously described settings (Subramanian et al., 2004, 2006). Expressed fusion proteins showed appropriate RLUC or YFP activity in onion cells and all YFP-tagged proteins localized to the nucleus. The Y:B ratio for each protein RLUC/YFP combination was calculated from at least three and up to 20 onion samples and statistical analysis performed using a Student's *t* test.

RT-PCR

RNA was isolated from root, whole seedling, and inflorescence tissue using an RNeasy kit (Qiagen) and cDNA generated from 1 μg RNA using an oligo(dT) primer with Superscript III reverse transcriptase (Invitrogen). The sequences of primers used to amplify cDNA are listed (see Supplemental Table 5 online). All cDNAs were amplified using a standard PCR cycle. Due to sequence identity, *SLK1* and *SLK3* PCR products are amplified by the same set of primers. Presence of an *Hpa*I site in the *SLK1* cDNA sequence, however, allows these PCR products to be distinguished following a restriction digest.

Microscopy

Scanning electron microscopy and in situ hybridization were performed as described previously (Golz et al., 2004). Digoxigenin-labeled probes were transcribed from a PCR fragment containing a portion of the *LUG*, *LUH*, *STM*, *PHB*, or *FIL* cDNA (details available upon request). Histological sections (2 or 4 μm) were made from gluteraldehyde-fixed material embedded in LR-white resin and stained with Toluidine Blue. GUS staining was performed by briefly fixing tissue in 90% acetone and then incubating tissue overnight in a 50 mM phosphate buffer containing 2 mM X-Gluc and a mixture of 3 mM potassium ferricyanide and ferrocyanide at 37°C. Tissue was either examined as whole mounts in 70% ethanol or embedded in Paraplast Plus, before being sectioned at 8 μm and viewed under DIC optics. Embryos within developing seeds were observed under DIC optics following treatment with Hoyer's solution. For fluorescence microscopy, developing seeds were placed in a 10% glycerol solution and pressure applied to force the embryo out of the seed.

Construction of Transgenic Plants Expressing amiRNAs

Primers for amiRNAs targeting *LUG* and *LUH* mRNA were designed according to WMD2 Web MicroRNA Designer (http://wmd2.weigelworld.org; Schwab et al., 2006). *amiR-LUG* (targets 2443 to 2463 bp of the *LUG* mRNA) and *amiR-LUH* (targets 437 to 457 bp of the *LUH* mRNA) were generated by sequential PCR using *miR-319a* as a template and subsequently placed downstream of the *35S* promoter in pART7 (Gleave, 1992). The $35S_{pro}$*:amiRNA* cassette was subcloned into pMLBART and introduced into *Arabidopsis* using procedures outlined above. To generate the FIL_{pro}*:amiR-LUG* construct, the *FIL* promoter (–3873 to –12 bp) was placed upstream of *amiR-LUG* and the whole cassette moved into pMLBART. *yab3* mutants segregating for *fil* were transformed using procedures outlined above and transgenic *fil yab3* plants identified in either the T1 or T2 populations. To create the Op_{pro}*:amiR-LUG* construct, *amiR-LUG* was placed downstream of six tandemly arranged *Operator* (*Op*) sequences in pBluescript (kindly provided by Ian Moore). The Op_{pro}*:amiR-LUG* cassette was then moved to pMLBART and introduced into

Arabidopsis lines expressing $AS1_{pro}$*:LhG4*. This combination was called $AS1_{pro}$*>>amiR-LUG*.

Phylogenetic Analysis

Inferred protein sequence was aligned using Clustal software and then manually adjusted to optimize alignments. PAUP software was then used to generate an unrooted phylogeny using the neighbor-joining method (Saitou and Nei, 1987) and nodes of the tree supported by bootstrap values generated from 1000 trials.

Accession Numbers

Sequence data of genes described in this article can be found in the Arabidopsis Genome Initiative library under the following accession numbers: *FIL* (NM_130082, At2g45190), *LUG* (NM_119407, At4g32551), *LUH* (NM_128829, At2g32700), *SEU* (NM_103511, At1g43850), *SLK1* (At4g25520), *SLK2* (NM_125602, At5g62090), *SLK3* (At4g25515), *YAB2* (At1g08465), *YAB3* (NM_116235, At4g00180), and *YAB5* (NM_128215, At2g26580). T-DNA insertion alleles and tilling mutant alleles described in this article were obtained from the ABRC using the following identifiers: SALK_126444 (*lug-444*), SALK_113012 (*lug-012*), SALK_097509 (*luh-4*), SALK_089954 (*slk2-1*), SALK_038662 (*slk2-2*), CS93680 (*yab2-1*), and CS90062 (*yab5-1*).

Supplemental Data

The following materials are available in the online version of this article.

Supplemental Figure 1. Floral Phenotypes of *fil lug* and *fil yab3 lug* Mutants.

Supplemental Figure 2. Vegetative Phenotypes of *yab* Mutants.

Supplemental Figure 3. Polarity Defects of *fil yab3 lug luh*/+ Leaves.

Supplemental Figure 4. RNA in Situ Hybridization Showing the Pattern of *LUG* and *LUH* Expression in Developing Embryos.

Supplemental Figure 5. Structure of T-DNA Insertion Alleles Used in This Study.

Supplemental Figure 6. Ectopic *KNOX* Expression in Mutants.

Supplemental Table 1. Defining the Dimerization Domain of FIL.

Supplemental Table 2. Interactions between SEU, SLK, and the Corepressors LUG and LUH in Yeast.

Supplemental Table 3. Dimensions of Wild-Type and Mutant Leaves.

Supplemental Table 4. Plant Material Used in This Study.

Supplemental Table 5. RT-PCR Primers Used in This Study.

Supplemental Data Set 1. Text File of the Alignment Used for the Phylogenetic Analysis Shown in Figure 7B.

ACKNOWLEDGMENTS

We thank C. Cobbett for critical reading of this manuscript. We are grateful to Z. Schwarz-Sommer for providing some of the yeast two-hybrid clones, P. Doerner, S. Hake, and M. Tucker for reporter lines, J. Bowman and V. Sundaresan for various *yab* mutants and driver lines, Belinda Appleton for help with phylogenetic analysis, and the ABRC stock center for other seed stocks used in this study. We also thank Gianna Romano, Marnie Soso, and Melanie Hutchins for genotyping plants and Rebecca Wilson for preliminary BRET analyses. This work was funded by the Australian Research Council (J.F.G.) and by National Science Foundation Grant DBI-0619631 (A.G.V.).

Received August 2, 2009; revised August 2, 2009; accepted September 28, 2009; published October 16, 2009.

REFERENCES

Aida, M., Ishida, T., Fukaki, H., Fujisawa, H., and Tasaka, M. (1997). Genes involved in organ separation in *Arabidopsis*: An analysis of the cup-shaped cotyledon mutant. Plant Cell **9:** 841–857.

Alvarez, J., and Smyth, D.R. (1999). *CRABS CLAW* and *SPATULA*, two *Arabidopsis* genes that control carpel development in parallel with *AGAMOUS.* Development **126:** 2377–2386.

Bowman, J.L., and Smyth, D.R. (1999). *CRABS CLAW*, a gene that regulates carpel and nectary development in *Arabidopsis*, encodes a novel protein with zinc finger and helix-loop-helix domains. Development **126:** 2387–2396.

Clough, S.J., and Bent, A.F. (1998). Floral dip: A simplified method for Agrobacterium-mediated transformation of *Arabidopsis thaliana.* Plant J. **16:** 735–743.

Conner, J., and Liu, Z. (2000). LEUNIG, a putative transcriptional corepressor that regulates AGAMOUS expression during flower development. Proc. Natl. Acad. Sci. USA **97:** 12902–12907.

Emery, J.F., Floyd, S.K., Alvarez, J., Eshed, Y., Hawker, N.P., Izhaki, A., Baum, S.F., and Bowman, J.L. (2003). Radial patterning of *Arabidopsis* shoots by class III *HD-ZIP* and *KANADI* genes. Curr. Biol. **13:** 1768–1774.

Eshed, Y., Baum, S.F., Perea, J.V., and Bowman, J.L. (2001). Establishment of polarity in lateral organs of plants. Curr. Biol. **11:** 1251–1260.

Eshed, Y., Izhaki, A., Baum, S.F., Floyd, S.K., and Bowman, J.L. (2004). Asymmetric leaf development and blade expansion in *Arabidopsis* are mediated by *KANADI* and *YABBY* activities. Development **131:** 2997–3006.

Franks, R.G., Liu, Z., and Fischer, R.L. (2006). SEUSS and LEUNIG regulate cell proliferation, vascular development and organ polarity in Arabidopsis petals. Planta **224:** 801–811.

Franks, R.G., Wang, C., Levin, J.Z., and Liu, Z. (2002). SEUSS, a member of a novel family of plant regulatory proteins, represses floral homeotic gene expression with LEUNIG. Development **129:** 253–263.

Gleave, A.P. (1992). A versatile binary vector system with a T-DNA organisational structure conducive to efficient integration of cloned DNA into the plant genome. Plant Mol. Biol. **20:** 1203–1207.

Goldshmidt, A., Alvarez, J.P., Bowman, J.L., and Eshed, Y. (2008). Signals derived from YABBY gene activities in organ primordia regulate growth and partitioning of *Arabidopsis* shoot apical meristems. Plant Cell **20:** 1217–1230.

Golz, J.F., Roccaro, M., Kuzoff, R., and Hudson, A. (2004). *GRAMINIFOLIA* promotes growth and polarity of *Antirrhinum* leaves. Development **131:** 3661–3670.

Greb, T., Clarenz, O., Schafer, E., Muller, D., Herrero, R., Schmitz, G., and Theres, K. (2003). Molecular analysis of the LATERAL SUPPRESSOR gene in Arabidopsis reveals a conserved control mechanism for axillary meristem formation. Genes Dev. **17:** 1175–1187.

Ha, C.M., Jun, J.H., Nam, H.G., and Fletcher, J.C. (2007). BLADE-ON-PETIOLE 1 and 2 control *Arabidopsis* lateral organ fate through regulation of LOB domain and adaxial-abaxial polarity genes. Plant Cell **19:** 1809–1825.

Hibara, K., Karim, M.R., Takada, S., Taoka, K., Furutani, M., Aida, M., and Tasaka, M. (2006). *Arabidopsis* CUP-SHAPED COTYLEDON3 regulates postembryonic shoot meristem and organ boundary formation. Plant Cell **18:** 2946–2957.

Kanaya, E., Nakajima, N., and Okada, K. (2002). Non-sequence-specific DNA binding by the FILAMENTOUS FLOWER protein from

Arabidopsis thaliana is reduced by EDTA. J. Biol. Chem. **277:** 11957–11964.

Kerstetter, R.A., Bollman, K., Taylor, R.A., Bomblies, K., and Poethig, R.S. (2001). *KANADI* regulates organ polarity in *Arabidopsis.* Nature **411:** 706–709.

Kim, M., Pham, T., Hamidi, A., McCormick, S., Kuzoff, R.K., and Sinha, N. (2003). Reduced leaf complexity in tomato wiry mutants suggests a role for *PHAN* and *KNOX* genes in generating compound leaves. Development **130:** 4405–4415.

Kumaran, M.K., Bowman, J.L., and Sundaresan, V. (2002). *YABBY* polarity genes mediate the repression of *KNOX* homeobox genes in *Arabidopsis.* Plant Cell **14:** 2761–2770.

Liu, Z., and Meyerowitz, E.M. (1995). LEUNIG regulates *AGAMOUS* expression in Arabidopsis flowers. Development **121:** 975–991.

McConnell, J.R., and Barton, M.K. (1998). Leaf polarity and meristem formation in *Arabidopsis.* Development **125:** 2935–2942.

McConnell, J.R., Emery, J.F., Eshed, Y., Bao, N., Bowman, J., and Barton, M.K. (2001). Role of *PHABULOSA* and *PHAVOLUTA* in determining radial patterning in shoots. Nature **411:** 709–713.

Navarro, C., Efremova, N., Golz, J.F., Rubiera, R., Kuckenberg, M., Castillo, R., Tietz, O., Saedler, H., and Schwarz-Sommer, Z. (2004). Molecular and genetic interactions between *STYLOSA* and *GRAMINIFOLIA* in the control of *Antirrhinum* vegetative and reproductive development. Development **131:** 3649–3659.

Otsuga, D., DeGuzman, B., Prigge, M.J., Drews, G.N., and Clark, S. E. (2001). *REVOLUTA* regulates meristem initiation at lateral positions. Plant J. **25:** 223–236.

Pekker, I., Alvarez, J.P., and Eshed, Y. (2005). Auxin response factors mediate *Arabidopsis* organ asymmetry via modulation of *KANADI* activity. Plant Cell **17:** 2899–2910.

Prunet, N., Morel, P., Thierry, A.M., Eshed, Y., Bowman, J.L., Negrutiu, I., and Trehin, C. (2008). REBELOTE, SQUINT, and ULTRAPETALA1 function redundantly in the temporal regulation of floral meristem termination in *Arabidopsis thaliana*. Plant Cell **20:** 901–919.

Saitou, N., and Nei, M. (1987). The neighbor-joining method: A new method for reconstructing phylogenetic trees. Mol. Biol. Evol. **4:** 406–425.

Sawa, S., Watanabe, K., Goto, K., Liu, Y.G., Shibata, D., Kanaya, E., Morita, E.H., and Okada, K. (1999). *FILAMENTOUS FLOWER*, a meristem and organ identity gene of *Arabidopsis*, encodes a protein with a zinc finger and HMG-related domains. Genes Dev. **13:** 1079–1088.

Schwab, R., Ossowski, S., Riester, M., Warthmann, N., and Weigel, D. (2006). Highly specific gene silencing by artificial microRNAs in Arabidopsis. Plant Cell **18:** 1121–1133.

Siegfried, K.R., Eshed, Y., Baum, S.F., Otsuga, D., Drews, G.N., and Bowman, J.L. (1999). Members of the *YABBY* gene family specify abaxial cell fate in *Arabidopsis.* Development **126:** 4117–4128.

Sitaraman, J., Bui, M., and Liu, Z. (2008). LEUNIG_HOMOLOG and LEUNIG perform partially redundant functions during Arabidopsis embryo and floral development. Plant Physiol. **147:** 672–681.

Sridhar, V.V., Surendrarao, A., Gonzalez, D., Conlan, R.S., and Liu, Z. (2004). Transcriptional repression of target genes by LEUNIG and SEUSS, two interacting regulatory proteins for *Arabidopsis* flower development. Proc. Natl. Acad. Sci. USA **101:** 11494–11499.

Subramanian, C., Kim, B.H., Lyssenko, N.N., Xu, X., Johnson, C.H., and von Arnim, A.G. (2004). The *Arabidopsis* repressor of light signaling, COP1, is regulated by nuclear exclusion: Mutational analysis by bioluminescence resonance energy transfer. Proc. Natl. Acad. Sci. USA **101:** 6798–6802.

Subramanian, C., Woo, J., Cai, X., Xu, X., Servick, S., Johnson, C.H., Nebenführ, A., and von Arnim, A.G. (2006). A suite of tools and application notes for in vivo protein interaction assays using bioluminescence resonance energy transfer (BRET). Plant J. **48:** 138–152.

Takada, S., Hibara, K., Ishida, T., and Tasaka, M. (2001). The *CUP-SHAPED COTYLEDON1* gene of Arabidopsis regulates shoot apical meristem formation. Development **128:** 1127–1135.

Villanueva, J.M., Broadhvest, J., Hauser, B.A., Meister, R.J., Schneitz, K., and Gasser, C.S. (1999). *INNER NO OUTER* regulates abaxial–adaxial patterning in *Arabidopsis* ovules. Genes Dev. **13:** 3160–3169.

Vroemen, C.W., Mordhorst, A.P., Albrecht, C., Kwaaitaal, M.A., and de Vries, S.C. (2003). The *CUP-SHAPED COTYLEDON3* gene is required for boundary and shoot meristem formation in Arabidopsis. Plant Cell **15:** 1563–1577.

Yamada, T., Ito, M., and Kato, M. (2004). YABBY2-homologue expression in lateral organs of *Amborella trichopoda* (Amborellaceae). Int. J. Plant Sci. **165:** 917–924.